JCTC Journal of Chemical Theory and Computation

Article

pubs.acs.org/JCTC

Physisorption, Diffusion, and Chemisorption Pathways of H_2 Molecule on Graphene and on (2,2) Carbon Nanotube by First Principles Calculations

Francesca Costanzo,* Pier Luigi Silvestrelli, and Francesco Ancilotto

Dipartimento di Fisica e Astronomia, Università di Padova, via Marzolo 8, I-35131 Padova, Italy, and CNR-IOM-DEMOCRITOS National Simulation Center, Trieste, Italy

ABSTRACT: We investigate the interaction of the H_2 molecule with a graphene layer and with a small-radius carbon nanotube using ab initio density functional methods. H_2 can interact with carbon materials like graphene, graphite, and nanotubes either through physisorption or chemisorption. The physisorption mechanism involves the binding of the hydrogen molecule on the material as a result of weak van der Waals forces, while the chemisorption mechanism involves the dissociation of the hydrogen molecule and the ensuing reaction of both hydrogen atoms with the unsatured C−C bonds to form C−H bonds. In our calculations, we take into account van der Waals interactions using a recently developed method based on the concept of maximally localized Wannier functions. We explore several adsorption sites and orientations of the hydrogen molecule relative to the carbon surface and compute the associated binding energies and adsorption potentials. The most stable physisorbed state on graphene is found to be the hollow site in the center of a carbon hexagon, with a binding energy of −48 meV, in good agreement with experimental results. The analysis of diffusion pathways between different physisorbed states on graphene shows that molecular hydrogen can easily diffuse at room temperature from one configuration to another, which are separated by energy barriers as small as 10 meV. We also compute the potential energy surfaces for the dissociative chemisorption of H_2 on highly symmetric sites of graphene, the lowest activation barrier found being 2.67 eV. Much weaker adsorption characterizes instead the physisorption interaction of the H_2 molecule with the small radius (2,2) CNT. The barriers for H_2 dissociation on the nanotube external surface are significantly lowered with respect to the graphene case, showing the remarkable effect of the substrate curvature in promoting hydrogen dissociation.

I. INTRODUCTION

Carbon-based nanomaterials like the carbon nanotube (CNT) and graphite have attracted much attention because of their suitability as materials for gas storage. In particular, the reported high hydrogen uptake in these materials makes them attractive for hydrogen storage devices in fuel-cell-powered electric vehicles.[1] Starting from the pioneering work of Dillon et al.,[2] who first reported the H_2 adsorption capacity of single-walled carbon nanotubes, many experimental and theoretical studies have been carried out to understand the adsorption mechanisms on carbon substrates.

The interaction of H_2 with graphene sheets has also been studied more recently, showing the capability of such carbon material to bind hydrogen on both side of its structure. Understanding the hydrogenation of graphene layers is important from several perspectives. For example, Elias et al.[3] demonstrated the reversible transition of graphene layers from semimetallic to semiconducting properties after hydrogenation. This is an important issue to promote the applications of graphene layers in microelectronics.

The hydrogen molecule may interact with carbon materials either by physisorption of the intact molecule or by chemisorption of the hydrogen atoms of the dissociated molecule. Understanding the interplay between molecular physisorption and atomic chemisorption would be useful for addressing the problem of hydrogen storage material. Physisorption of hydrogen molecules on graphene has been examined using density functional theory (DFT), suggesting binding energies on the order of 80−90 meV.[4,5] The importance of an accurate description of the van der Waals (vdW) interactions for physisorption processes cannot be overemphasized. In the present work, we take into account vdW interactions using the DFT/vdW-WF method,[6,7] based on the concept of maximally localized Wannier functions. This technique, as discussed in the following, combines the simplicity of the semiempirical formalism with the accuracy of the first principles approaches.

The capability of a graphene sheet to bind molecular hydrogen via vdW forces will be compared with that of the (2,2) "armchair" carbon nanotube. This system, which is the smallest radius carbon nanotube available, is chosen here to emphasize the role of curvature of the carbon substrate in determining the hydrogen adsorption properties. In particular, as explained in the following section, we find that the dissociation energy barrier for the H_2 molecule decreases by a factor of 3 on graphene with respect to the isolated molecule and by a factor of 10 on the (2,2) CNT surface, showing the favorable effect of the curvature of the carbon material to promote dissociation.

Finally, we compare the results of our method with the results obtained using different, alternative recipes to include the vdW interactions.[8−12]

Received: February 17, 2012
Published: March 19, 2012

   dx.doi.org/10.1021/ct300143a | J. Chem. Theory Comput. 2012, 8, 1288−1294

II. METHODS

A. DFT Calculations. First principles calculations have been carried out within the Car−Parrinello approach[13] in the framework of density functional theory (DFT), using the PBE exchange-correlation functional.[14] Although PBE often provides reasonable estimates for the interaction energy in weakly bound systems due to a favorable, partial error cancellation, this agreement should be considered accidental, due to the well-known inability of DFT to reproduce genuine vdW effects. Nevertheless, the PBE approach including vdW interactions have been recently applied for the binding/diffusion of hydrogen atoms on graphene.[15,16] Also, the bare PBE functional has been successfully used in the calculations of H diffusion on semiconducting, metallic, and transition-metal surfaces like Si(110),[17] titanium nitride (TiN),[18] and Fe(111) surfaces,[19] as well as in magnesium nanostructures[20] or Ni- and Ti-doped Mg(0001) surfaces.[21] We will describe below our own recipe to correct DFT results in order to properly include vdW interactions. Only valence electrons were treated explicitly in our calculations, and interactions with the ionic cores were described by using norm-conserving pseudopotentials generated according to the prescription of Troullier and Martins.[22] The Kleinman−Bylander[23] decomposition was used for the C species, with s and p nonlocality. H atoms were represented instead by a simple s-type pseudopotential. Periodic boundary conditions were used, and only the Γ point was considered in the Brillouin zone integration. The Kohn−Sham orbitals were expanded in plane waves up to an energy cutoff of 70 Ry, which is sufficient to yield converged structural properties for the investigated systems.

To model the graphene surface, a periodically repeated slab model with a single layer of 32 C atoms was chosen. The symmetry of the cell was hexagonal, with parameters a = 18.6 bohr, $b = a$, and c = 46.5 bohr.

To model the (2,2) CNT, we used a rolled-up graphene sheet with 32 carbon atoms and a diameter of 2.85 Å, aligned with the z axis. The symmetry of the cell was tetragonal with a = 30 bohr, $b = a$, and c = 18.9 bohr. Due to our use of periodic boundary conditions along z, we effectively consider an infinite tube (with metallic electronic properties). The chosen a and b values for the transverse size of the supercell are large enough to avoid any spurious interactions between periodic replica of the nanotube.

As already mentioned before, a known drawback of standard DFT methods concerns their failure to describe vdW interactions, and in particular the leading term $-C_6/R^6$, which results from dipole−dipole electron correlation effects. An adequate treatment of these effects is nonetheless essential to the study of physisorption states that are weakly bonded configurations where vdW dispersion interactions play a key role. We overcame the DFT limitations by applying the DFT/vdW-WF method reported in full detail in refs 6 and 7. The method is based on the generation of the maximally localized Wannier functions (MLWFs) and uses as the only input the ground state Kohn−Sham orbitals computed in the conventional DFT approach. The MLWFs, a generalization of the localized Boys' orbitals[24] for systems characterized by periodic boundary conditions, allow the total electronic density to be partitioned into individual fragment contributions, in a chemically transparent fashion. Once the MLWFs are obtained, the leading $-C_6/R^6$ correction terms are evaluated by using suitable expressions for long-range interactions between separated fragments of matter.[6,25] The method has been already successfully applied to small molecules, bulk, and surface systems.[6,26]

To confirm our results and to further test our method, we have also calculated vdW corrections with other methods like the so-called "seamless" vdW-DF method,[27] based on a fully nonlocal dispersion energy functional, and a semiempirical approach, namely the DFT-D method,[28] which consists of adding a $-C_6/R^6$ dispersion correction to the conventional Kohn−Sham DFT energy, the vdW interactions being described via a simple pairwise force field. We performed all of the calculations with the CPMD program. To use the vdW-DF method, we performed additional DFT calculations by using the Quantum-ESPRESSO ab initio package, where this method is implemented. With Quantum-ESPRESSO,[29] ultrasoft pseudopotentials were adopted, and the generalized gradient approximation (GGA), in the PBE flavor,[14] was used for the exchange-correlation energy.

III. RESULTS AND DISCUSSION

We consider first the adsorption of an intact, isolated hydrogen molecule on a planar graphene sheet. We performed several calculations for the graphene−hydrogen system, with variable separation between the graphene sheet and the hydrogen molecule's center of mass. Different adsorption sites were considered, with the axis of the hydrogen molecule aligned either parallel or perpendicular to the graphene surface. We considered adsorption on hollow (H, in the center of the carbon hexagon), top (T, on top of the carbon atom), and bridge (B, above the midpoint of the C−C bond) sites. Figure 1

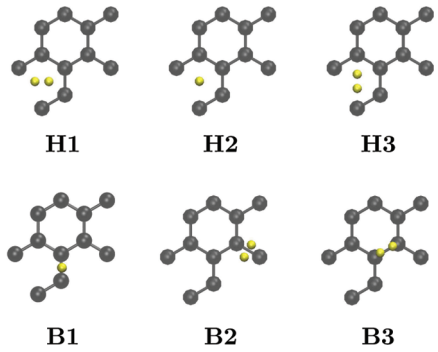

Figure 1. Physisorbed configuration sites for H_2 on graphene. H and B stand for hollow and bridge sites, respectively.

shows the six configurations of the H_2 molecule in the H and B configurations. Figure 2 shows instead the T configurations. Configurations H3, B3, T1, and T4 have the H_2 molecular axis parallel to a C−C bond. H2, B1, and T5 have the H_2 molecular axis perpendicular to the graphene sheet. H1 and B2 have the H_2 molecular axis oriented parallel to the plane and perpendicular to the C−C bond of the graphene sheet. The remaining top configurations T2 and T3 have the H_2 molecular

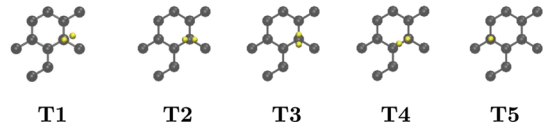

Figure 2. Physisorbed configurations sites for H_2 on graphene. T stands for top site.

dx.doi.org/10.1021/ct300143a | J. Chem. Theory Comput. 2012, 8, 1288−1294

axis parallel to the graphene sheet and forming angles of 30° and 60°, respectively, with respect to the underlying C−C bond.

We computed the total energies of the hydrogen−carbon systems for different configurations, where the separation z between the carbon substrate and the center of mass of the H_2 molecule was varied between 2 and 7 Å, thus allowing for the computation of the adsorption potential $V(z)$ in the relevant separation range and for the location of the energy minimum value and position. The adsorption potential is defined as $V(z) = E_{tot} - (E_{substrate} + E_{H_2})$, where $E_{substrate,H_2}$ represents the energies of the isolated fragments (the substrate, either graphene or the CNT, and the hydrogen molecule), and E_{tot} is the energy of the interacting system when the separation between the substrate and the center of mass of the H_2 molecule is equal to z. Consequently, the binding energy is defined as $E_b = V(z_{min})$, where z_{min} is the equilibrium molecule−substrate distance.

Figure 3 shows $V(z)$ on the H3 site, as computed using different approximations. The higher energy curve represents

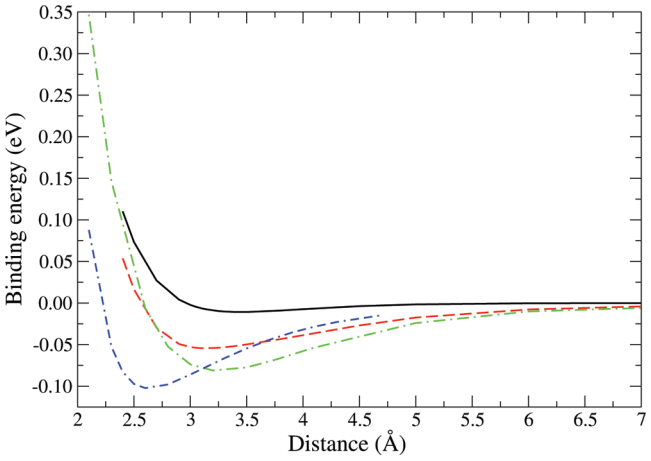

Figure 3. Physisorption of H_2 on graphene, in the hollow configuration. Pure DFT calculations are indicated by a solid line, DFT/vdW-WF results by a long-dashed line, vdW-DF by a dashed-dotted line, and DFT-D by a dashed−dashed−dotted line.

the results of the pure DFT calculations. When vdW interactions are taken into account with the various methods described in the previous section, the calculated adsorption potentials become more attractive, the values at the minimum increasing by 30−40 meV in absolute value with respect to the pure DFT results. The curve obtained by the DFT/vdW-WF method,[6] in particular, gives a binding energy E_b of −54 meV with a minimum at a distance of 3.2 Å.

We compare our result with the experimental estimate of −47.6 meV for the lowest energy level of physisorbed H_2 as measured by Mattera et al.[30] The original measurements of ref 30 were performed on a graphite substrate. We corrected the experimental result to adapt it to the case of graphene by subtracting the extra binding due to the second, third, etc. layers underneath the graphene sheet; to compute such contributions, we used a simple yet sufficiently accurate empirical pair potential[31] describing the C−H_2 interaction, thus arriving at the −47.6 meV value quoted above. In order to compare our results with this experimental value, we must correct E_b by adding the quantum zero-point energy of the adsorbed H_2 molecule, which we found, by numerically solving the Schrodinger equation in the adsorption potential $V(z)$, to be about 6 meV. The corrected value, −48 meV, is in very good agreement with the experimental result mentioned above. The results obtained with other methods, in particular the semiempirical DFT-D approach[28] and the "seamless" method,[27] overestimate the interaction between the graphene and the H_2 molecule and are not in a good agreement with the experimental value;[30] in fact, DFT-D[28] calculation gives a binding energy of −98 meV at 2.8 Å, while vdW-DF[27] predicts a binding energy of −81 meV at 3.2 Å.

Table 1 reports, for all of the configurations studied, the binding energy E_b and the equilibrium distance as computed

Table 1. Minimum Energy Distances z_{min} (Å) and Binding Energies (meV) for the Physisorbed States of H_2 Molecule on Graphene, Shown in Figures 1 and 2

	z_{min}	DFT	z_{min}	DFT/vdW-DFT
T1	3.4	+25	3.2	−13
T2	3.6	−9	3.6	−43
T3	3.5	−9	3.4	−39
T4	3.6	−9	3.4	−46
T5	3.1	−10	3.1	−38
H1	3.4	−10	3.0	−48
H2	3.5	−11	3.5	−47
H3	3.5	−11	3.2	−54
B1	3.3	−8	3.3	−43
B2	3.6	+2	3.6	−35
B3	3.6	−9	3.6	−43

with pure DFT and with DFT/vdW-WF. Looking at the pure DFT results (third column), one can notice that DFT does not permit one to easily discriminate, among the three hollow configurations (H1, H2, and H3), the most stable one, while adding the vdW interactions clearly favors the H3 configuration. This result is in agreement with Henwood and Carey,[32] although the comparison can be only qualitative since these authors neglected vdW corrections in their DFT calculations. The DFT/vdW-WF results are in reasonable agreement with those obtained by more sophisticated quantum-chemistry methods like CCSD[37] and MP2.[8]

The diffusion barriers ΔE_{barr} for the hydrogen molecule moving across the surface from the most stable configuration H3 have been calculated as the difference between the initial physisorbed state and the transition state, which is either a B or a T site. ΔE_{barr} is about 10 meV for H configurations (H3 and H1) diffusing on the graphene surface through the B (B3 and B2) configurations. Similar ΔE_{barr} values have been calculated for displacement across the T site directly above a carbon atom. The barriers found are rather low, and hence the physisorbed molecules are expected to be quite mobile on graphene at, e.g., room temperature.

As anticipated in the Introduction, one of the aims of this work is to study the effect of the curvature of the carbon sheet on the interaction with hydrogen molecules. We considered for simplicity the extreme case of a system with maximum curvature, i.e., a (2,2) CNT, which is the smallest radius nanotube realizable ($R \approx 1.5$ Å), and we studied the physisorption of H_2 on the external surface of it. We considered adsorption on the hollow (H3) site (i.e., in the center of the carbon hexagon) and on the B3 site (i.e., above the C−C bond and with the molecule axis parallel to it).

Table 2 reports, for the two configurations studied of H_2 on (2,2) CNT, the binding energy E_b and the equilibrium distance

Table 2. Minimum Energy Distances z_{min}(Å) and Binding Energy (meV) for the Physisorbed States of H_2 Molecule on (2,2) CNT, Shown in Figure 4

	z_{min}	DFT	z_{min}	DFT/vdW-DFT
H3	4.3	−6	3.9	−30
B3	4.6	−5	4.0	−27

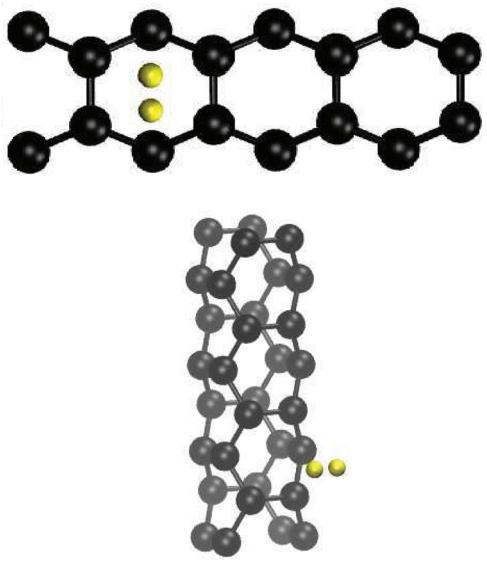

Figure 4. Physisorbed H_2 on the (2,2) armchair nanotube in the H3 configuration. Top and side views are drawn.

as computed with pure DFT and with DFT/vdW-WF. Figure 4 shows the (2,2) CNT with the H_2 molecule in the H3 configuration (which we find to be the lowest energy physisorbed structure) outside the nanotube. Figure 5 shows the associated adsorption potentials computed with the pure

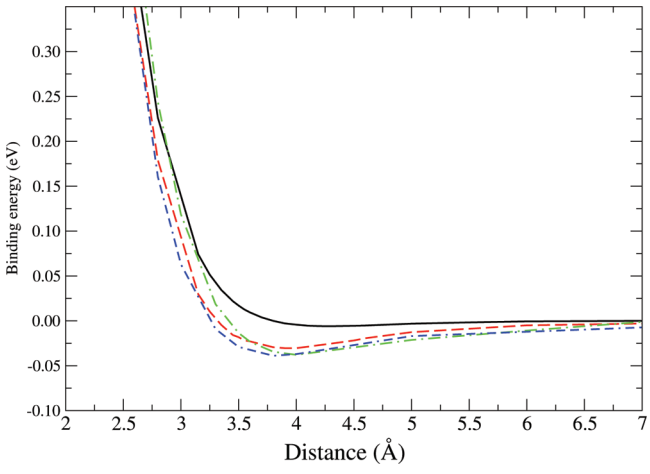

Figure 5. Physisorption of H_2 on the (2,2) nanotube, hollow configuration. Pure DFT calculations are indicated by a solid line, DFT/vdW-WF results by a long-dashed line, vdW-DF by a dashed-dotted line, and DFT-D by a dashed−dashed−dotted line.

DFT and including vdW interactions with the three methods: DFT/vdW-WF, vdW-DF, and vdW-D. From the results of Figure 5, it appears that the DFT gives a binding energy (not corrected for zero-point motion) of −6 meV while DFT/vdW-WF gives a binding energy of −30 meV, i.e., a factor 2 smaller than the calculated binding energy on graphene. Both vdW-DF and vdW-D predict instead a binding energy of −38 meV. All of the methods agree to place the minimum energy position at about 4.0 Å from the nanotube surface.

We next studied the chemisorbed states of hydrogen on both graphene and the CNT surface. Atomic hydrogen can strongly bind to a C atomic site, provided the H_2 molecule undergoes dissociation. Relevant information in this respect is the energy barriers separating the initial physisorbed state from the transition state (TS) and the energy of the final configuration where the two H atoms are chemically bound to the carbon surface. To investigate the minimum energy pathway for the hydrogen dissociative adsorption on graphene, we used the Nudge Elastic Band (NBE)[33] method in our calculations.

Figure 6 shows the three possible chemisorbed configurations of H_2 atoms on graphene after molecular dissociation.

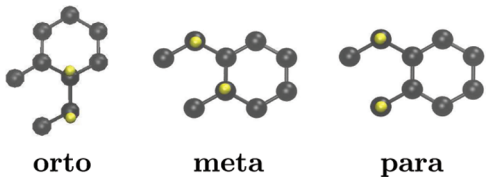

Figure 6. Chemisorbed state of the dissociated H_2 molecule on graphene. Orto, meta, and para refer to the position of the hydrogen atoms in the ring.

The energetically favored configuration is found when two H atoms are adsorbed on the opposite vertices (para position) of the same hexagon ring of graphene, as shown in the right panel of Figure 6. This result is consistent with those of Miura et al. and Ao and Li.[9,34] The C−H bond length in the para configuration is 1.12 Å. The C atoms beneath the two H atoms move up by about 0.32 Å, with a distortion of a dihedral angle of 30°, while the C−C bond length elongates to 1.51 Å. This is similar to the sp^3 bond length of diamond (1.53 Å), while it is larger than the value for the sp^2 carbon bond length (1.42 Å). The reconstruction of the graphene layer was also reported by Miura et al.,[9] who predicted that the C atoms bonded with the H atoms move out of the graphene plane by 0.35 Å,[9] changing from sp^2 to sp^3-like character.

Figure 7 shows the pathway calculated for H3 → para chemisorption of H_2 on graphene. It appears that the energy of the final, dissociated configuration is higher than that of the physisorbed one, thus characterizing this hydrogenation process as an endothermic reaction. This path connecting the H3 configuration to the para configuration has the lowest energy barrier, 2.62 eV. Table 3 reports all of the energy barriers for the explored paths from physisorbed to chemisorbed states for H_2 on both the graphene and the (2,2) CNT surfaces. The transition state TS is characterized by a broken H−H bond and by the formation of a new C−H bond (1.14 Å length), with a substantial distortion of the carbon substrate. In fact, the dihedral angle varies from 180° from the pristine graphene to 163° in the hydrogenated graphene.

Similar results have been obtained in the recent work of McKay et al.,[10] where they also showed that applying an

dx.doi.org/10.1021/ct300143a | J. Chem. Theory Comput. 2012, 8, 1288−1294

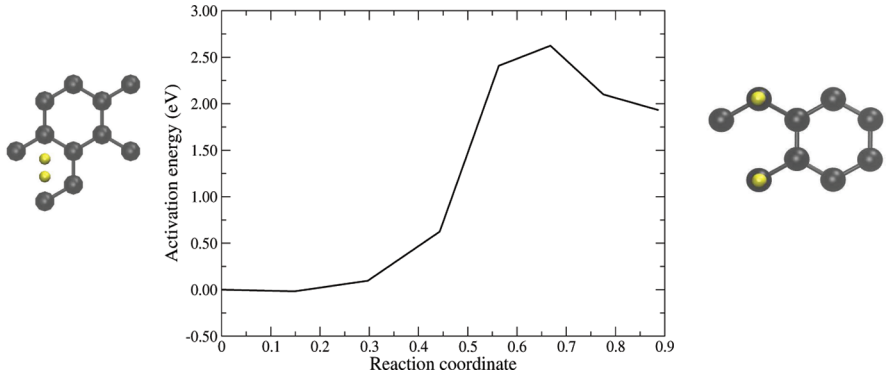

Figure 7. Chemisorption reaction path of H_2 on graphene, from the H3 physisorbed state to the para chemisorbed state.

Table 3. Activation Barriers for the H_2 Dissociation

H_2 on graphene	ΔA (eV)
H1 → meta	3.86
H3 → meta	3.57
H3 → para	2.62
H3 → orto	3.33
B3 → orto	3.6
H_2 on (2,2) CNT	ΔA (eV)
B3 → orto	0.76
H3 → para	1.26

external stress to the graphene substrate can lower the barrier for dissociation by a factor of 6 and change the process from endothermic to exothermic. We will show in the following that a similar effect is achieved by increasing the curvature of the carbon substrate, i.e., adsorbing hydrogen on the surface of a small-radius CNT.

We calculated the reaction pathways from the B3 physisorbed state to the orto chemisorbed state on the CNT. Figure 8 shows the existence of an activation energy barrier of 0.76 eV. The effective repulsion between the two adjacent hydrogen atoms, which makes this structure energetically unfavored in graphene (−43 and −54 meV for B3 and H3, respectively, see also Table 1), is reduced here by the curvature of the nanotube, resulting in a more distant H−H pair. Remarkably, the C−C bond directly below the chemisorbed H atoms is stretched from 1.42 to 1.67 Å. This value, which is definitely larger than a typical single bond in, e.g., diamond (1.53 Å), is closer to the "world's longest carbon−carbon bond" (1.704 Å) recently created in carefully designed alkane molecules.[35]

Figure 9 shows the reaction path between the H3 physisorbed state (which has a slightly higher binding energy than the B3 state) and the para chemisorbed state, characterized by an energy barrier about 0.5 eV higher than the one for the B3-orto reaction path described above (see Table 3).

While the dissociation process of H_2 on graphene was found to be endothermic (see Figure 7), in the case of small-radii CNT, it turns out to be exothermic, as discussed above. This is due to the higher reactivity of the dangling bonds of the carbon atoms in the sp^3 hybridization state that characterizes the local carbon structure of the (2,2) CNT. Similar results were obtained by Scipioni et al.[36] in the case of a completely hydrogenated (2,2) CNT, with only two free C atom positions available for the hydrogen molecule dissociation. At variance with the results of ref 36, where free energy barriers of 1.5−2.0 eV are found at 300 and 600 K, respectively, we find for the clean CNT a much lower dissociation barrier (see Figure 8).

A. CONCLUSIONS

We explored several adsorption sites and the orientation of hydrogen molecule relative to the graphene plane. The most stable physisorbed state is in the hollow site, with a binding energy of −48 meV. This value, which is obtained using the DFT/vdW-WF approach to include vdW interactions, is in good agreement with experimental results. The analysis of diffusion paths among physisorbed states shows that molecular hydrogen can easily diffuse on graphene at room temperature

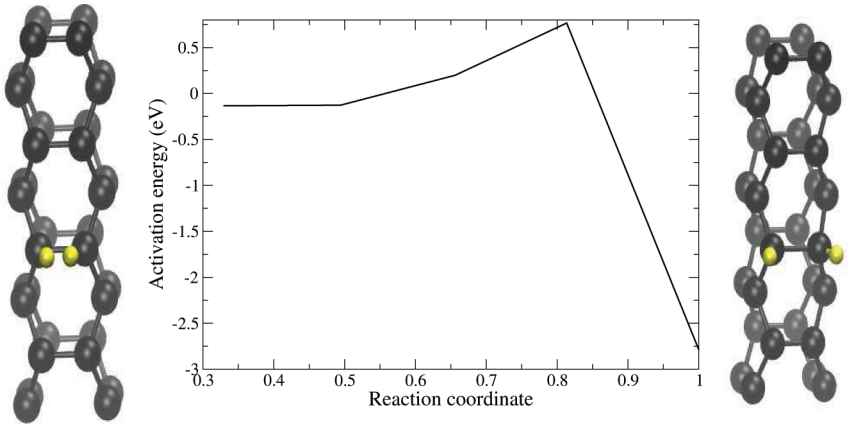

Figure 8. Chemisorption reaction path of H_2 on the (2,2) CNT, from the B3 physisorbed state to the orto chemisorbed state.

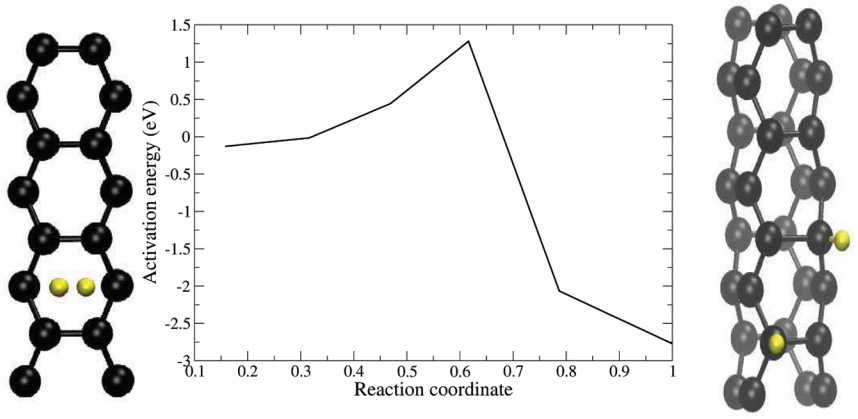

Figure 9. Chemisorption reaction path of H_2 on the (2,2) CNT, from the H3 physisorbed state to the para chemisorbed state.

across sites separated by energy barriers as small as 10 meV. Much weaker binding characterized instead the physisorbed state of the hydrogen molecule on the surface of a (2,2) CNT. The situation is different when the hydrogen molecules approach the carbon surface (G or CNT) and dissociate. In particular, we calculated the potential energy surfaces for the dissociative adsorption of H_2 on highly symmetric sites of graphene (orto, meta, and para positions). The lowest activation barrier of 2.67 eV is that one that corresponds to the transition from the H_2 physisorbed state to the para chemisorbed state. Other energy paths are characterized by higher activation barriers (3.0 eV and above). Moreover, the effect of the curvature of the (2,2) CNT confirms the catalytic effect of the surface in the dissociation process of H_2 molecule,[36] which turns from endothermic (on graphene) to exothermic with an activation barrier of 0.76 eV. Our results strongly confirm the importance of including accurate vdW interactions for studying these systems.[8,11]

AUTHOR INFORMATION

Corresponding Author

*Telephone: +39-049-8277251. E-mail: fcostanz@pd.infn.it.

Notes

The authors declare no competing financial interest.

ACKNOWLEDGMENTS

We thank Roberto Scipioni for useful comments and suggestions.

REFERENCES

(1) Geim, A. K. Graphene: Status and Prospects. *Science* **2009**, *324*, 1530−1534.

(2) Dillon, A. C.; Jones, K. M.; Bekkedahl, T. A.; Kiang, C. H.; Bethune, D. S.; Heben, M. J. Storage of hydrogen in single-walled carbon nanotubes. *Nature* **1997**, *386*, 377−379.

(3) Elias, D. C.; Nair, R. R.; Mohiuddin, T. M. G.; Morozov, S. V.; Blake, P.; Halsall, M. P.; Ferrari, A. C.; Boukhvalov, D. W.; Katsnelson, M. I.; Geim, A. K.; Novoselov, K. S. Control of Graphene's Properties by Reversible Hydrogenation: Evidence fro Graphene. *Science* **2009**, *323*, 610−613.

(4) Okamoto, Y.; Miyamoto, Y. Ab Initio Investigation of Physisorption of Molecular Hydrogen on Planar and Curved Graphenes. *J. Phys. Chem. B* **2001**, *105*, 3470−3474.

(5) Arellano, J. S.; Molina, L. M.; Rubio, A.; Alonso, J. A. Density functional tudy of adsorption of molecular hydrogen on graphene layers. *J. Chem. Phys.* **2000**, *112*, 8114−8119.

(6) Silvestrelli, P. L. Van der Waals Interactions in DFT Made Easy by Wannier Functions. *Phys. Rev. Lett.* **2008**, *100*, 053002−4.

(7) Silvestrelli, P. L. van der Waals Interactions in Density Functional Theory Using Wannier Functions. *J. Phys. Chem A* **2009**, *113*, 5224−5234.

(8) Rubeš, M.; Bludský, O. DFT/CCSD(T) Investigation of the Interaction of Molecular Hydrogen with Carbon Nanostructures. *Chem. Phys. Chem* **2009**, *10*, 1868−1873.

(9) Miura, Y.; Kasai, H.; Diño, W.; Nakanishi, H.; Sugimoto, T. First principles studies for the dissociative adsorption of H2 on graphene. *J. Appl. Phys.* **2003**, *93*, 3395−3400.

(10) McKay, H.; Wales, D. J.; Jenkins, S. J.; Verges, J. A.; de Andres, P. L. Hydrogen on graphene under stress: Molecular dissociation and gap opening. *Phys. Rev. B* **2010**, *81*, 075425−6.

(11) Du, A. J.; Smith, S. C. Van der Waals-corrected density functional theory: benchmarking for hydrogen-nanotube and nanotube-nanotube interactions. *Nanotechnology* **2005**, *16*, 2118−2123.

(12) Lu, Y.; Feng, Y. P. Adsorptions of hydrogen on graphene and other forms of carbon structures: First principle calculations. *Nanoscale* **2011**, *3*, 2444−2453.

(13) Car, R.; Parrinello, M. Unified Approach for Molecular Dynamics and Density-Functional Theory. *Phys. Rev. Lett.* **1985**, *55*, 2471−2474.

(14) Perdew, J. P.; Burke, K.; Ernzerhof, M. Generalized Gradient Approximation Made Simple. *Phys. Rev. Lett.* **1996**, *77*, 3865−3868.

(15) Ma, J.; Michaelides, A.; Alfe, D. Binding of hydrogen on benzene, coronene, and graphene from quantum Monte Carlo calculations. *J. Chem. Phys.* **2011**, *134*, 134701−6.

(16) Ma, J.; Michaelides, A.; Alfe, D.; Schimka, L.; Kresse, G.; Wang, E. Adsorption and diffusion of water on graphene from first principles. *Phys. Rev. B* **2011**, *84*, 033402−4.

(17) Brázdová, V.; Bowler, D. R. H atom adsorption and diffusion on Si(110)-(1x1) and (2x1) surfaces. *Phys. Chem. Chem. Phys.* **2011**, *13*, 11367−11372.

(18) Marlo, M.; Milman, V. Density-functional study of bulk and surface properties of titanium nitride using different exchange-correlation functionals. *Phys. Rev. B* **2000**, *62*, 2899−2907.

(19) Huo, C.-F.; Li, Y.-W.; Wang, J.; Jiao, H. Surface Structure and Energetic of Hydrogen Adsorption on the Fe(111) Surface. *J. Phys. Chem. B* **2005**, *109*, 14160−14167.

(20) Du., A. J.; Smith, S. C.; Yao, X. D.; He, Y.; Lu, G. Q. Atomic Hydrogen Diffusion in Novel Magnesium Nanostructures: The Impact of Incorporated Subsurface Carbon Atoms. *J. Phys.: Conf. Ser.* **2006**, *29*, 167−172.

(21) Pozzo, M.; Alfe, D.; Amieiro, A.; French, S.; Pratt, A. Hydrogen dissociation and Diffusion on Ni- and Ti-doped Mg(0001) surfaces. *J. Chem. Phys.* **2008**, *128*, 094703−11.

(22) Troullier, N.; Martins, J. L. Efficient pseudopotentials for plane-wave calculations. *Phys. Rev B* **1991**, *43*, 1993−2006.

(23) Kleinman, L.; Bylander, D. M. Efficacious Form for Model Pseudopotentials. *Phys. Rev. Lett.* **1982**, *48*, 1425−1428.
(24) Boys, S. F.; Bernardi, F. The calculation of small molecular interactions by the differences of separate total energies. Some procedures with reduced errors. *Mol. Phys.* **1970**, *19*, 553−566.
(25) Andersson, Y.; Langreth, D. C.; Lundqvist, B. I. van der Waals Interactions in Density-Functional Theory. *Phys. Rev. Lett.* **1996**, *76*, 102−105.
(26) Silvestrelli, P. L.; Benyahia, K.; Grubisiĉ, S.; Ancilotto, F.; Toigo, F. Van der Waals interactions at surfaces by density functional theory using Wannier functions. *J. Chem. Phys.* **2009**, *130*, 074702−4.
(27) Dion, M.; Rydberg, H.; Schröder, E.; Langreth, D. C.; Lundqvist, B. I. Van der Waals Density Functional for General Geometries. *Phys. Rev. Lett.* **2004**, *92*, 246401−4.
(28) Grimme, S. Accurate Description of van der Waals Complexes by Density Functional Theory Including Empirical Corrections. *J. Comput. Chem.* **2004**, *25*, 1463−1473.
(29) Giannozzi, P.; et al. QUANTUM ESPRESSO: a modular and open-source software project for quantum simulations of materials. *J. Phys.: Condens. Matter* **2009**, *21*, 395502−19.
(30) Mattera, L.; Rosatelli, R.; Salvo, C.; Tommasini, F.; Valbusa, U.; Vidali, G. Selective adsorption of $^1H_2$ and $^2H_2$ on the (0001) graphite surface. *Surf. Sci.* **1980**, *93*, 515−525.
(31) Crowell, A. D.; Brown, J. S. Laterally averaged interaction potentials for 1H2 and 2H2 on the (0001) graphite surface. *Surf. Sci.* **1982**, *123*, 296−304.
(32) Henwood, D.; Carey, D. J. Ab initio investigation of molecular hydrogen physisorption on graphene and carbon nanotubes. *Phys. Rev. B* **2007**, *75*, 245413−10.
(33) Henkelman, G.; Jónsson, H. Improved tangent estimate in the nudged elastic band method for finding minimum energy paths and saddle points. *J. Chem. Phys.* **2000**, *113*, 9978−9985.
(34) Ao, Z.; Li, S. Hydrogenation of Graphene and Hydrogen Diffusion Behavior on Graphene/Graphane Interface. In *Graphene Simulation*; Gong, J. R., Ed.; Intech: August, 2011; Chapt. 4, pp 53−74.
(35) Schreiner, P. R.; Chernish, L. V.; Gunchenko, P. A.; Tikhonchuk, E. Y.; Hausmann, H.; Serafin, M.; Schlecht, S.; Dahl, J. E. P.; Carlson, R. M. K.; Fokin, A. A. Overcoming lability of extremely long alkane carbon-carbon bonds through dispersion forces. *Nature* **2011**, *477*, 308−311.
(36) Scipioni, R.; Boero, M.; Ohno, T. Hydrogenation of ultrasmall carbon nanotubes: A first principle study. *Chem. Phys. Lett.* **2009**, *480*, 215−219.
(37) Kostov, M. K.; Cheng, H.; Cooper, A. C.; Pez, G. P. Influence of Carbon Curvature on Molecular Adsorptions in Carbon-Based Materials: A Force Field Approach. *Phys. Rev. Lett.* **2002**, *89*, 146105−4.
(38) Marx, D.; Hutter, J. Ab Initio Molecular Dynamics: Theory and Implementation. *Mod. Methods Algorithms Quant. Chem.* **2000**, *3*, 329−477.
(39) Becke, A. D. Density-functional thermochemistry. III. The role of exact exchange. *J. Chem. Phys.* **1993**, *98*, 5648−5.